

## Exploring physiological diversity in *Vitis* genotypes: hydraulic traits in vines for oenological purposes and vines for table grapes

Emilio Villalobos-Soublett<sup>1</sup>, Marco Garrido-Salinas<sup>2</sup>, Nicolás Verdugo-Vásquez<sup>3</sup>, and Reinaldo Campos-Vargas<sup>4</sup>

<sup>1</sup> Programa de Doctorado en Ciencias Silvoagropecuarias y Veterinarias, Campus Sur, Universidad de Chile, Santiago 8820808, Chile.

<sup>2</sup> Departamento de Agronomía, Facultad de Ciencias, Universidad de la Serena, Avenida La Paz 1108, Ovalle, Chile. Postal code 1842646.

<sup>3</sup> Instituto de Investigaciones Agropecuarias, INIA Intihuasi. Colina San Joaquín s/n, La Serena, Chile.

<sup>4</sup> Centro de Estudios Postcosecha, Facultad de Ciencias Agronómicas, Universidad de Chile, Santiago 8831314, Chile.

**Abstract.** This study evaluates the physiological responses of table grape and wine grape genotypes under irrigated conditions in Northern Chile, aiming to identify hydraulic differences between purposes. Four table grape cultivars ('Flame Seedless', 'INIA-G3', 'INIA-G4', 'Alisson Seedless') and five wine grape cultivars ('Cabernet Franc', 'Chardonnay', 'Sauvignon Blanc', 'Moscatel de Alejandría', and a naturalized genotype) were compared. Using ANOVA and principal component analysis (PCA), significant differences were found in traits such as turgor loss point, stomatal density, leaf gas exchange, and water use efficiency. Results suggest that grapevines for oenological purposes tend to have higher water use efficiency and traits related to water retention, while table grapes are associated with higher stomatal conductance and water transport. The PCA emphasizes the contribution of hydraulic traits to the differentiation on grapevine genotypes, offering insights into how these traits may influence in water use. The study highlights phenotypic diversity within the species and suggests that specific traits providing drought tolerance may exist among table grape cultivars due to their selective breeding for high productivity, often at the expense of significant water use.

### 1. Introduction

Chile is one of the world's leading producers and exporters of both wine and table grapes. The country has a well-established viticulture industry that benefits from its Mediterranean climate and diverse terroirs, which are ideal for grape production. However, the increasing occurrence of extreme climatic conditions, including prolonged droughts, presents significant challenges for viticulture, particularly in hyper-arid regions [1]. In this context, understanding the hydraulic traits that determine water deficit tolerance in *Vitis vinifera* L. becomes crucial for developing management strategies and selecting more resilient cultivars. Recent studies have highlighted the importance of integrating multiple hydraulic traits to characterize drought tolerance in grapevines. These traits describe characteristics related to how plants manage the hydration of their cells, which is controlled through underlying physiological mechanisms [2,3,4]. However, more studies are needed to fully understand the intraspecific variability of these traits among *Vitis vinifera*,

especially in the case of table grapes. This study aims to explore how table grape genotypes perform in comparison to wine grape genotypes, specifically to broaden and discriminate the variability in their hydraulic traits.

### 2. Material and Methods

#### 2.1. Experimental site

The experiment was conducted during the 2023-2024 growing season at the Biodiversity Study Center of the Agricultural Research Institute (INIA) in Vicuña, located in the Coquimbo Region of Chile (30°02'16"S, 70°41'40"W, at an altitude of 634 m.a.s.l.). The climate of the site is classified as hyper-arid since it rains lower than 100 mm per year and concentrates in winter (June-September). The soil belongs to the sandy loam alluvial Entisol and has a flat topography (<1%). A soil sample taken from a depth of 0 to 30 cm exhibited the following composition: sand (54.1%), silt (28%), clay (17.85%), with volumetric water content at field capacity and wilting

point were 11.2% v v<sup>-1</sup> and 5.72% v v<sup>-1</sup>, respectively. The soil pH was 7.3, indicating a calcareous nature. Organic matter content was 1.5%, and electrical conductivity in saturated paste was 2.3 dS/m.

## 2.2. Experimental design and plant material

A completely randomized split-plot design was implemented. The structure consisted of the arrangement of 6 continuous and independent plots, of which the two central plots were utilized for the study. Within each plot, 18 subplots were carefully subdivided, each housing 9 genotypes of *V. vinifera*. The two central plots were randomly assigned to the main treatments, ensuring spatial variability was minimized, with four replications for each genotype achieved within the subplots. The grapevine genotypes used in this study included table grape cultivars: ‘Flame Seedless’ (FL), ‘INIA-G3’ (G3), ‘INIA-G4’ (G4), and ‘Allisson Seedless ®’ (Ali); and wine grape cultivars: ‘Cabernet Franc’ (CF), ‘Chardonnay’ (CH), ‘Sauvignon Blanc’ (SB), ‘Muscat of Alexandria’ (M. Ale), and ‘Naturalized genotype’ (NN). These genotypes are phylogenetically distant, as determined by previously conducted phylogenetic cluster analyses and confirmed through subsequent verification (data not shown). All plants used in the experiment were obtained from a nursery and were maintained under these conditions for one year in pots of 735 cm<sup>3</sup> under shaded conditions. The plants, approximately 20 cm in height and 2.8 ± 0.05 cm in diameter were established into the experimental field at the end of the 2023-2024 season (DOY 51) with a spacing of 1 x 1.5 m in north-south oriented rows and tied on a steel guide. The vines were drip irrigated using one irrigation line per row, with emitters spaced at 1 m intervals (1 emitter per plant), delivering water at a rate of 4 L/h. These emitters were positioned on the soil surface, ~10-15 cm away from the base of the trunk.

## 2.3. Measurements and estimates

### 2.3.1. Pressure-Volume Curves (PVC) and leaf mass area

For all replicates, a fully developed leaf was cut, rehydrated in distilled water, and kept under darkness conditions overnight for being measured the following day (DOY 71) using the bench-dry method (Sack and Pasquet-Kok, 2011). Leaf water potential was measured with a pressure chamber (Model 600D; PMS Instrument Company, Albany, USA). Leaves were measured until obtained at least 10 water potential-leaf fresh mass points. From PVC, values for water potential at turgor loss point (TLP), osmotic potential at full turgor ( $\pi_0$ ), and absolute leaf capacitance at full turgor ( $C_{leaf}$ ) were obtained following Sack and Pasquet-Kok (2011). The same leaves used for PVC were used to calculate the Specific leaf area (SLA = leaf area per unit leaf dry weight). Fresh leaf areas were measured using a CI-202 Portable Laser Leaf Area Meter (CID Bio-Science, Washington, USA). Then, the leaves were placed in an oven at 70 °C until constant

weight and their dry weight was measured on a precision balance.

### 2.3.2. Leaf gas exchange

On DOY 58 and 79, a portable infrared gas analyzer (LI-6400xt, LI-COR INC., Lincoln, Nebraska, United States) was used to measure stomatal conductance ( $g_s$ ), net CO<sub>2</sub> assimilation ( $A_n$ ), and leaf transpiration ( $E$ ) in grapevines. Well-developed healthy and sunlit leaves were selected from each vine. Leaves were carefully cleaned to remove any surface residues. During measurements, environmental conditions within the measurement chamber (temperature, relative humidity, and CO<sub>2</sub> concentration) were adjusted to match experimental field conditions. The molar air flow rate inside the leaf chamber was set to 500 mmol mol<sup>-1</sup>. Measurements were taken at a reference CO<sub>2</sub> concentration similar to the ambient environment (380–400 mmol mol<sup>-1</sup>). A natural saturating photosynthetic photon flux ensured leaves received more than 1.000  $\mu\text{mol m}^{-2} \text{s}^{-1}$ , preserving the leaf angle during measurement without the use of external light sources. The leaf intrinsic water use efficiency (WUE<sub>i</sub>) was calculated as the ratio of  $A_n$  to  $g_s$ .

### 2.3.3. Stomata density

Mature, fully developed leaves, along with adjacent leaves sampled during gas exchange measurements, were selected from each replicate. A thin layer of clear nail polish was applied to a 1 cm<sup>2</sup> area on the abaxial (lower lateral right lobe) surface of the leaf and allowed to dry completely. A piece of clear adhesive tape was placed over the dried nail polish, pressed gently to ensure adhesion, and then carefully peeled off to lift the nail polish imprint. The tape with the nail polish imprint was attached to a microscope slide, ensuring it was flat and free of air bubbles. The slide was examined under an optical microscope (Zeiss-Axio Lab.A1, USA) at 100x magnification and saved as an image (1 per replicate). The number of stomata within an image of view was counted using a neural network for automatic stomata identification and counting (<https://stomata.uvm.edu/>; Fetter et al., 2019). The stomatal density was calculated by dividing the total number of stomata by the total area observed.

### 2.3.4. Leaf hydraulics

The bench dehydration method was conducted two months after the plants were established in the field (DOY 87). The leaf hydraulic conductance was estimated through the partial rehydration method [5], as follows:

$$K_{leaf} = C_{leaf} [\ln(\Psi_0/\Psi_f)] / t \quad (1)$$

where  $C_{leaf}$  is the absolute leaf capacitance (mmol m<sup>-2</sup> MPa<sup>-1</sup>),  $\Psi_0$  and  $\Psi_f$  are leaf water potentials before and after partial rehydration (-MPa), respectively, and  $t$  is

rehydration time (s). Random samples of plants with sufficiently developed shoots, in terms of size and leaf number, were taken and analyzed for each genotype. A total of 10 shoots were collected for each genotype. The shoots, which were mostly lignified and approximately 1.5 meters long, were harvested in the morning around 6:00 a.m. (low xylem tension) and transported to the laboratory. To ensure maximum stem hydration, the plants were thoroughly watered the evening before collection. To ensure correct tissue hydration, branches were immediately put in distilled water and left hydrating and covered with opaque plastic bags for at least two hours. Before each measurement, branches were put in opaque plastic bags for 10–30 min to obtain water potential equilibrium, minimizing differences in water potential between leaves of the same branch. From each branch, two adjacent leaves were selected. The first leaf was sampled to measure  $\Psi_0$  using a pressure chamber (model 1505D EXP, PMS Instrument Company, Albany, NY, USA). Immediately afterward, the adjacent leaf was cut with the petiole under water leaving the leaf rehydrating for 30 s ( $t$ ; equation (1)). After that,  $\Psi_f$  was measured. These measurements were repeated during a bench dehydration period until the difference between  $\Psi_0$  and  $\Psi_f$  was minimal (<0.5 MPa), assuming a minimum leaf hydraulic conductance. Each  $K_{leaf}$  point was estimated with two leaves (between 24 and 36 leaves measured per genotype), and  $C_{leaf}$  (equation (1)) was estimated from Pressure-Volume Curves (PVC) made from independent samples.

#### 2.4. Statistical analysis

All analyses were computed in R v.3.5.2. The differences between genotypes and purposes were tested using a one-way ANOVA with Tukey honestly significant difference post hoc test with a significance level of 0.05. Linear Pearson correlations were performed between traits and linear regression was made for relevant relations. Both had a significance level of 0.05. In addition, Principal Component Analysis (PCA) was used to obtain a hierarchy of the variables analyzed to find patterns in the data and to classify any combination of variables that could explain the effects of genotypes and purposes. In each genotype, a Weibull function (Ogle et al., 2009) (Equation (2)) was adjusted to the relationship between leaf hydraulic conductance ( $K_{leaf}$ ) and a leaf water potential, by using the fitplc R package [6]. Thus, water potential in which 12%, 50%, and 88% ( $P_{12}$ ,  $P_{50}$ , and  $P_{88}$ , respectively) of the maximum leaf conductance ( $K_{max}$ ) are lost was determined. Parameters were estimated through Bootstrap methods.  $K_{max}$  was estimated through the average of the five highest  $K_{leaf}$  values of each genotype.

$$K = K_{max} \{ [1 - (X/100)] \}^{\{ [(\Psi_{xyl}/\Psi_x) ((\Psi_x - S_x)/V)] \}} \quad (2)$$

where  $K_{max}$  is the maximum leaf hydraulic conductance,  $\Psi_{xyl}$  is the xylem water potential,  $\Psi_x$  is the xylem water potential where  $x\%$  of the conductance is lost,  $S_x$  is the slope of the curve at  $\Psi_{xyl} = \Psi_x$ , and  $V$  is a function setting parameter. Also, the percent loss of conductivity (PLC)

was determined as the method proposed by Jacobsen and Pratt (2012):

$$PLC = 100 \times [1 - (K/K_{max})] \quad (3)$$

To test the effects of the genotypes or productive purpose on plant hydraulics, we used the water potential gradient and evapotranspiration to calculate the whole-plant hydraulic conductance as follows:

$$K_{plant} = [E/(\Psi_{pd} - \Psi_{leaf})] \quad (4)$$

where  $E$  represents the transpiration rate, and  $\Psi_{pd}$  and  $\Psi_{leaf}$  refer to predawn and leaf water potential, respectively, both of which were measured using a pressure chamber (Model 600D; PMS Instrument Company, Albany, USA).  $\Psi_{pd}$  was measured between 05:00 and 06:00 h, while  $\Psi_{leaf}$  was measured between 12:00 and 14:00 h (solar noon; Coordinated Universal Time UTC-3). For these measurements, mature, healthy, sun-exposed leaves were selected. The  $\Psi_{leaf}$  measurements were taken from the same leaves used for gas exchange measurements.

The relationship between both productive purposes was determined by principal component analysis (PCA) and the dissimilarity was determined by hierarchical cluster analysis (HCA; complete linkage method and Euclidean distance).

### 3. Results and discussion

The experiment occurred during predominantly hot and dry atmospheric conditions, without rainfall. January exhibited the highest temperatures and evapotranspiration rates, while February and March brought cooler, more humid conditions (Table 1).

**Table 1.** Meteorological data for the experimental site in Vicuña (January to March 2024): minimum air temperature ( $T_{min}$ ), mean temperature ( $T_{mean}$ ), maximum air temperature ( $T_{max}$ ), reference evapotranspiration ( $ET_0$ ), precipitation (pp).

Month	$T_{min}$ (°C)	$T_{mean}$ (°C)	$T_{max}$ (°C)	HR (%)	$ET_0$ (mm)	pp (mm)
January	11.8	21.2	32.1	57.2	6.3	0.0
February	12.8	20.8	30.7	65.1	5.3	0.0
March	10.7	19.8	30.7	61.4	4.4	0.0

The variations in  $\pi_0$  and TLP among genotypes, as well as when grouped by their purpose, is shown in Figure 1. Although the genotypes did not show significant differences in osmotic potential, with values ranging between -0.8 and -1.1 MPa (figure 1, A), wine grapes (Oeno) exhibited a consistent trend toward more negative osmotic potentials (figure 1, B). TLP varies both among genotypes and according to their purpose, with values

ranging from -1.0 to -1.3 MPa. CH and NN exhibit the lowest TLP values, while FL shows the highest TLP values. In this regard, there is a trend toward physiological differences between table grape and wine grape genotypes in their ability to regulate water and maintain turgor pressure, even under well-watered field conditions. However, these differences may become more pronounced under water stress [7].

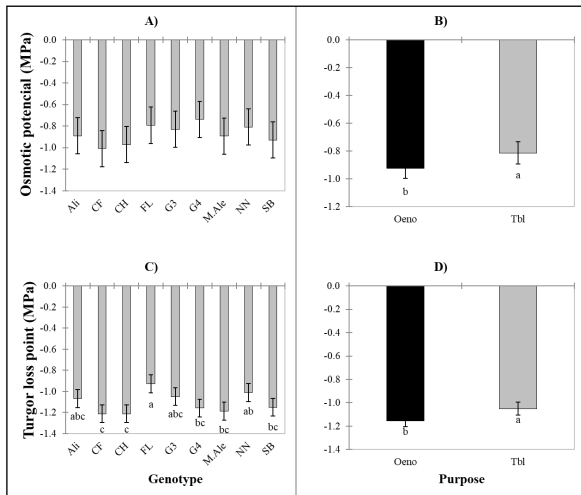


**Figure 1.** Leaf parameters derived from pressure-volume curves for different *V. vinifera* genotypes and their purposes (Oenological: Oeno; Tablegrapes: Tbl): Leaf osmotic potential at full turgor (A and B) and water potential at turgor loss point (C and D). For each genotype, n = 4; Tbl, n = 16; Oeno, n = 20. Different letters indicate significant differences among genotypes or purposes according to Tukey's post hoc test ( $p < 0.05$ ).

The genotypes exhibit significant variations across all leaf gas exchange parameters evaluated, with the most notable differences observed in  $g_s$  and E. The significantly higher  $WUE_i$  in Oenological genotypes ( $55.7 \mu\text{mol CO}_2 \text{ mmol}^{-1} \text{ H}_2\text{O}$ ) compared to Table grape genotypes ( $43.1 \mu\text{mol CO}_2 \text{ mmol}^{-1} \text{ H}_2\text{O}$ ) can be explained by their lower  $g_s$  and E, which allow for a more efficient use of water while maintaining  $A_n$  (Table 2). In contrast, table grape genotypes exhibit a higher stomatal density, which may enhance gas exchange under well-irrigated conditions where the focus is on maintaining optimal plant water status to promote fruit quality traits, such as berry size (figure 2; C and D). However, this higher stomatal density could reduce water use efficiency, particularly under water-limited conditions. Additionally, the lack of differences in SLA between genotypes and purposes suggests that leaf structure does not play a major role in these physiological differences, at least in young, irrigated plants under field conditions (figure 2; A and B). Instead, regulating leaf gas exchange through stomatal density and conductance seems to be a key factor driving the distinct water use strategies between table and wine grape genotypes.

The water potential at which leaf hydraulic conductance was reduced by 50% ( $P_{50}$ ) exhibited considerable variability among genotypes (Figure 2). These values ranged from -1.90 MPa (G3) to -0.94 MPa (Ali), both of which are table grape genotypes (Table 2). Under the conditions of this study with young, well-watered plants, the  $P_{50}$  values were lower than the TLP values, showing a

good correlation ( $R^2 = 0.64$ ), and were generally lower than those reported for some of the genotypes in previous studies [8]. Further seasons of study are required, as these values are expected to decrease as the plants age and as each growing cycle progresses within a single season. This trend is likely due to the decreasing threshold of hydraulic vulnerability with plant maturation and the cumulative effects of environmental stressors over time [9].

**Table 2.** Differences between genotype and purpose on leaf gas exchange: Means of net photosynthetic rate ( $A_n$ ;  $\mu\text{mol CO}_2 \text{ m}^{-2} \text{ s}^{-1}$ ), stomatal conductance ( $g_s$ ,  $\text{mol H}_2\text{O m}^{-2} \text{ s}^{-1}$ ), transpiration rate (E;  $\text{mmol H}_2\text{O m}^{-2} \text{ s}^{-1}$ ), and intrinsic water use efficiency ( $WUE_i$ ;  $\mu\text{mol CO}_2 \text{ mol}^{-1} \text{ H}_2\text{O}$ ).

Genotype	$A_n$	$g_s$	E	$WUE_i$
NN	13.9 ab	0.31 ab	7.6 ab	48.1 ab
Allisson Seedless	13.3 ab	0.36 a	8.1 a	40.0 b
Chardonnay	14.3 a	0.24 ab	7.0 abc	62.2 ab
Moscatel de Alejandria	13.3 ab	0.27 ab	7.0 abc	52.3 ab
INIA-G4	12.5 ab	0.31 ab	7.3 ab	44.1 ab
INIA-G3	12.8 ab	0.30 ab	7.9 ab	38.3 b
Cabernet Franc	11.7 ab	0.19 b	5.7 c	66.0 a
Flame Seedless	11.1 b	0.23 ab	6.8 abc	50.0 ab
Sauvignon Blanc	12.1 ab	0.23 ab	6.4 bc	49.7 ab
Purpose				
Oenological	13.0 a	0.25 b	6.7 b	55.7 a
Tablegrapes	12.4 a	0.30 a	7.4 a	43.1 b
Pr > F(Genotype)	0.02	0.04	0.00	0.01
Pr > F(Purpose)	0.21	0.04	0.03	0.00

The values correspond to the average of two dates evaluated. For each genotype, n = 4; Tbl, n = 16; Oeno, n = 20. Means followed by the same letter are not significantly different at the 5% level according to Tukey's test.

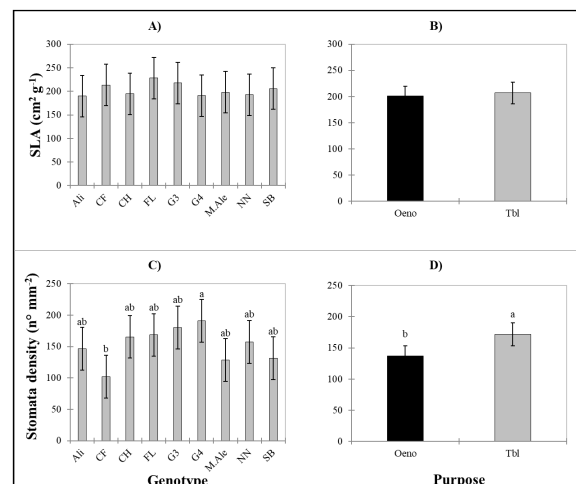


**Figure 2.** Specific leaf area (SLA) (A and B) and Stomata density (C and D) for different *V. vinifera* genotypes and their purposes (Oenological: Oeno; Tablegrapes: Tbl). For each genotype, n = 4; Tbl, n = 16; Oeno, n = 20. Different letters indicate significant differences among genotypes or purposes according to Tukey's post hoc test ( $p < 0.05$ ).

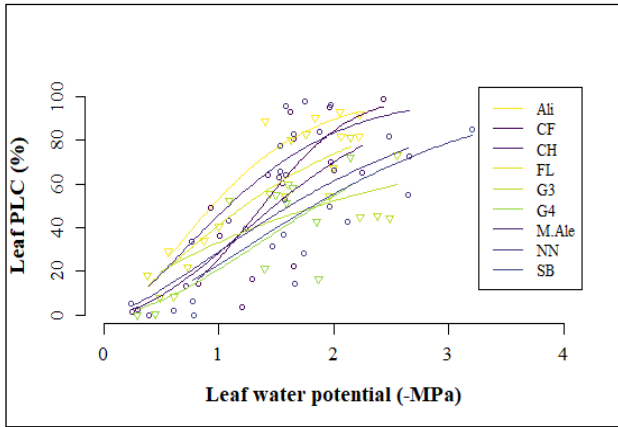


**Figure 3.** Leaf hydraulic conductance vulnerability curves for nine *V. vinifera* genotypes, categorized by purpose. Oenological genotypes (circles, purple gradient) and table grape genotypes (inverted triangles, green gradient) are represented.

**Table 2.** The water potential at which leaf hydraulic conductance was reduced by 50% ( $P_{50}$ ), and the slope of the relationship between leaf hydraulic conductance and leaf water potential ( $S_x$ ), for nine *V. vinifera* genotypes.

Genotype	P50 (MPa)	Boot-2.5%	Boot-97.5%	SX	Boot-2.5%	Boot-97.5%
Allisson Seedless	-0.94	0.77	1.14	57.6	48.3	97.5
Cabernet Franc	-1.38	1.07	1.67	66.1	36.7	259.3
Chardonnay	-1.48	1.20	1.74	43.0	31.2	211.8
Flame Seedless	-1.22	1.07	1.41	37.8	24.8	50.7
INIA-G3	-1.86	1.3	2.42	16	-	28.8
INIA-G4	-1.86	1.54	2.81	32.6	8.3	139.9
Moscatel de Alejandria	-1.08	0.64	1.41	49.3	29.3	128.8
NN	-1.61	0.94	2.40	31.6	9.8	264.1
Sauvignon Blanc	-1.82	1.42	2.26	30.7	17.6	58.7

The principal component analysis (PCA) presented in figure 4 illustrates the relationships between various physiological traits across different grapevine genotypes. The first two principal components, F1 and F2, account for 40.17% and 27.84% of the total variance, respectively. This analysis includes both oenological (wine grape) and table grape genotypes, represented by circles and triangles, respectively. Traits such as water-use efficiency (WUEi), leaf gas exchange parameters, and hydraulic properties are projected as vectors to indicate their contributions to the separation among genotypes. According to the PCA, the variables that contribute the most to F1 and axis F2 are  $g_s$  and TLP, respectively. Genotypes such as CF, SB, and CH are positioned closely together, suggesting similarities in their physiological traits, particularly those associated with WUEi and  $P_{50}$ . In contrast, genotypes such as G3 and FL are separated along the F1 axis, indicating differences in traits such as stomatal density (StoDen) TLP. The findings

suggest that different genotypes employ diverse water-use strategies, likely driven by trade-offs between water efficiency and productivity.

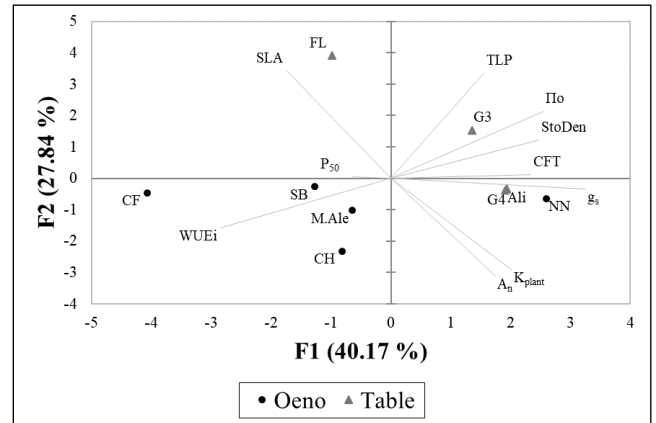


**Figure 4.** Principal Component Analysis of Physiological Traits in Wine and Table Grape Genotypes. Oenological genotypes (circles) and table grape genotypes (triangles) are represented.

#### 4. Conclusions

Physiological differences were identified between table and wine grape genotypes, particularly in traits related to water-use efficiency, stomatal conductance, and hydraulic properties. Wine grape genotypes exhibited higher water-use efficiency, likely attributed to their lower stomatal conductance, enabling better water conservation under irrigated conditions. In contrast, table grape genotypes displayed traits favoring greater water transport and gas exchange, likely driven by selective breeding for fruit size and yield. These distinct water-use strategies highlight the phenotypic diversity within *Vitis vinifera*. Given the extensive genetic variation within the species, it remains challenging to delineate clear differences in vulnerability based on production purposes. Molecular approaches could provide valuable insights into the mechanisms underlying this variability. Furthermore, future research should focus on examining these physiological traits under varying levels of water stress, particularly in table grape genotypes, to improve irrigation water management and promote sustainable production in the face of increasing water scarcity.

#### 5. References

- G.V. Jones, E.J. Edwards, M. Bonada, V.O. Sadras, M.P. Krstic, M.J. Herderich. *Managing wine quality* (Elsevier), pp. 728–741 (2022).
- S. Dayer, J.C. Herrera, Z. Dai, R. Burlett, L.J. Lamarque, S. Delzon, G. Bortolami, H. Cochard, G.A. Gambetta. *J. Exp. Bot.* 71, 4333–4344 (2020).
- G.A. Gambetta, J.C. Herrera, S. Dayer, Q. Feng, U. Hochberg, S.D. Castellarin. *J. Exp. Bot.* 71(16), 4658–4676 (2020).

4. S. Dayer, L.J. Lamarque, R. Burlett, G. Bortolami, S. Delzon, J.C. Herrera, G.A. Gambetta. *Plant Physiol.* 190(3), 1673–1686 (2022).
5. T.J. Brodribb, N.M. Holbrook, E.J. Edwards, M.V. Gutiérrez. *Plant Cell Environ.* 26(3), 443–450 (2003).
6. R.A. Duursma, B. Choat. *J. Plant Hydraul.* 4, e002 (2017). <http://doi.org/10.20870/jph.2017.e002>
7. G. Charrier, S. Delzon, J.C. Domec, L. Zhang, C.E. Delmas, I. Merlin, G.A. Gambetta. *Sci. Adv.* 4(1), eaao6969 (2018).
8. M.K. Bartlett, G. Sinclair. *J. Exp. Bot.* 72(5), 1995–2009 (2021).
9. Y. Sorek, S. Greenstein, Y. Netzer, I. Shtein, S. Jansen, U. Hochberg. *New Phytol.* 229(4), 1955–1969 (2021).